Synthetic fractional flux quanta in a ring of superconducting qubits

Luca Chirolli [1,*] Juan Polo [1] Gianluigi Catelani [1,2] and Luigi Amico [1,3,4]

[1] *Quantum Research Center, Technology Innovation Institute, Abu Dhabi 9639, United Arab Emirates*
[2] *JARA Institute for Quantum Information (PGI-11), Forschungszentrum Jülich, 52425 Jülich, Germany*
[3] *Dipartimento di Fisica e Astronomia "Ettore Majorana", Via S. Sofia 64, 95123 Catania, Italy*
[4] *INFN-Sezione di Catania, Via S. Sofia 64, 95127 Catania, Italy*

(Received 5 October 2024; accepted 11 September 2025; published 24 October 2025)

A ring of capacitively coupled transmons threaded by a synthetic magnetic field is studied as a realization of a strongly interacting bosonic system. The synthetic flux is imparted through a specific Floquet modulation scheme based on a suitable periodic sequence of Lorentzian pulses that are known as "Levitons." Such scheme has the advantage to preserve the translation invariance of the system and to work at the qubit sweet spots. We employ this system to demonstrate the concept of fractional values of flux quanta. Although such fractionalization phenomenon was originally predicted for bright solitons in cold atoms, it may be in fact challenging to access with that platform. Here, we show how fractional flux quanta can be read out in the absorption spectrum of a suitable "scattering experiment" in which the qubit ring is driven by microwaves.

DOI: 10.1103/d3rk-kh1k

I. INTRODUCTION

Networks of mesoscopic-scale systems at sufficiently low temperature can provide us with artificial quantum matter that can be exploited both to study fundamental aspects of quantum science and to design quantum devices [1]. To this end, different platforms have been explored, ranging from arrays of quantum dots [2] and trapped ions [3] to superconducting circuits [4] and cold atoms [5,6]. A fruitful viewpoint adopted so far in the community has been that genuine notions of mesoscopic physics of electronic systems such as the Josephson effect, point contacts, or persistent currents can provide inspiration to define concepts in quantum technology [7–12]. Here, we provide a case study going in the opposite direction: We demonstrate that specific notions originally emerging in current research in quantum technology, as in ultracold atoms systems, can inspire electronic mesoscopic physics. Specifically, we will refer to attractive bosonic cold atoms [13–17]. On one hand, such systems are difficult to simulate classically. On the other hand, attracting bosons allow the formation of bright solitons that, in turn, bear a great potential in atomtronics and quantum sensing [10–12]. In particular, bright solitons in a one-dimensional lattice have peculiar properties of stability [18], which are predicted to have a strong impact in interferometry [19].

Here, we focus on a striking property of lattice bright solitons confined in a ring-shaped potential pierced by a synthetic magnetic field: As a result of specific many-body correlations, the system's persistent current is characterized by a periodicity reflecting a fractional value with respect to the flux quantum Φ_0 obtained in the noninteracting case. Crucially for the logic we adopt in the present work, we note that the fractionalization phenomenon manifests itself in a fractional periodicity of the energies of the system as a function of the magnetic field, which, following Leggett, are the analogue of Bloch bands for the problem [20]. In the present case, such fractionalization is predicted to scale as the inverse of the number of particles N_p in the system [21]. Such N_p dependence makes it difficult to directly observe the feature in cold atom experiments, since N_p is typically large.

In this work, we will define a superconducting qubit quantum simulator for the dynamics of attracting bosons hosted in a ring lattice pierced by an *effective magnetic field*. In particular, we shall see that our system displays signatures of the fractionalization phenomenon distinctive for bright solitons. *Linear* chains of capacitivelly coupled qubits have been realized experimentally and have aroused considerable interest in the fields of driven-dissipative dynamics [22], many-body localization [23–26], disordered quantum phases of artificial matter [27], quantum walks [28–30], and perfect quantum state transfer [31,32]. In these systems, the low-energy modes are plasmons that can be excited by microwave photons and propagate through the capacitors. Such excitations behave as bosons located at the qubit's sites, and because of the nonlinear inductance of the Josephson junctions in the qubits, they can interact with each other. In contrast to the Cooper pair dynamics occurring in Josephson junctions arrays [33], here the boson-boson interaction is effectively *attractive* [34,35]. The important observation, here, is that the natural regime in which such systems work is the one of moderate number of bosons N_p, thus opening the door for analyzing the attractive Bose-Hubbard dynamics [18,36–38] in conditions that might be challenging to reach in other physical platforms.

[*] Contact author: luca.chirolli@unifi.it

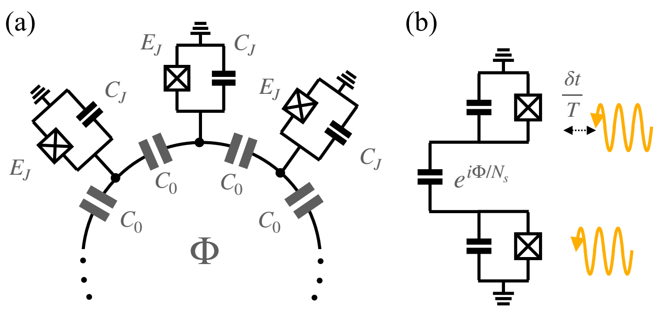

FIG. 1. (a) Schematics of a circuit constituted by a chain of transmons, which realizes an attractive Bose-Hubbard model. (b) Floquet modulation protocol, consisting in local transmon frequency modulation.

Our capacitively coupled qubit ring system is depicted in Fig. 1(a). In particular, we note that the effective magnetic field cannot induce any actual matter-wave motion as it occurs, for example, in cold atoms. Nevertheless, we can implement a synthetic magnetic field in our superconducting qubit system through a Floquet driving [39–43] of the transmon frequencies. The latter is suitably engineered to facilitate the operations to be carried out on the superconducting circuit system and protect the transmon performances from decoherence.

II. SYSTEM AND METHODS

Transmons are weakly anharmonic quantum oscillators that are well described by attractive bosons [34,35]. The latter consist of collective oscillations in the circuit and the attraction results from the weak anharmonicity provided by the Josephson potential in the regime $E_J \gg E_C$, with E_J the Josephson energy and E_C the charging energy. In a ring configuration with N_s capacitively coupled transmons, as schematized in Fig. 1, the bosonic excitations can hop from one transmon to the other and realize a Bose-Hubbard model of attractive bosons in a lattice [27,44,45]:

$$H_0 = \sum_{j=1}^{N_s} \left[\omega n_j - \frac{U}{2} n_j(n_j - 1) - J_0(a^\dagger_{j+1} a_j + \text{H.c.}) \right], \quad (1)$$

where $a_{N_s+1} \equiv a_1$, $n_j = a^\dagger_j a_j$, $\omega \simeq \sqrt{8E_C E_J} - E_C$, $U \simeq E_C$, $J_0 \simeq (C_0/(C_J + C_g))\sqrt{E_C E_J/8}$, and we set $\hbar = 1$ henceforth. The charging energy of the transmons $E_C = e^2/(2(C_J + C_g))$ is expressed in terms of the capacitance of the Josephson junction C_J and the capacitance to ground of the superconducting islands C_g, with $C_0 \ll C_J, C_g$ being the capacitance between nearest-neighbor transmons. Assuming $(C_0/(C_J + C_g))\sqrt{E_J/(8E_C)} \ll 1$, we have $J_0 \ll U \ll \omega$ (see Ref. [46] for details on the circuit Hamiltonian), implying strongly attractive interaction. We note that the transmon frequency can be modulated $\omega \to \omega(t)$ by employing the so-called split junctions, composed by a parallel of Josephson junctions threaded by a time-dependent external flux $\varphi_x(t)$. Special working points are the so-called sweet spots that correspond to maxima or minima of the energy versus φ_x. In this regime, the qubit properties are particularly stable against flux noise [4,47–49].

Synthetic gauge fields can be realized experimentally through Floquet modulation protocols [39–42]. The modulation is described by time-dependent frequencies $\omega_j(t) = \omega - \delta\omega_j(t)$, where $\delta\omega$ is periodic with period T and we assume $2\pi/T \gg J_0, U$. Therefore, the Hamiltonian acquires an additional term

$$H(t) = H_0 - \sum_j \delta\omega_j(t) n_j. \quad (2)$$

We can perform the unitary transformation $U(t) = \exp[i \sum_j n_j \int^t dt' \delta\omega_j(t')]$ so that the effective Floquet Hamiltonian in the fundamental band is given by the time-averaged Hamiltonian $H_{\text{eff}} = \langle U^\dagger(t) H(t) U(t) - i U^\dagger(t) \dot{U}(t) \rangle_T$, with $\langle \cdots \rangle_T \equiv \int_0^T \frac{dt}{T} \cdots$. The goal of the protocol is that H_{eff} acquires a complex hopping amplitude $J_0 \to J_0 e^{i\frac{\Phi}{N_s}}$, accounting for the Peierls substitution employed in one-dimensional matterwave circuits in the presence of a gauge field [50]. A finite Peierls phase has been achieved in two-dimensional arrays of transmons in the hardcore boson limit ($U \to \infty$) with a combination of static gradients and local sinusoidal modulations of ω that match the gradient steps [23,51,52]. We notice that such protocol typically lifts the transmons away from their sweet spot and that in the absence of static gradients, a sinusoidal driving has been demonstrated to yield generic values of Peierls phases in $\{0, 2\pi\}$ at the price of suitably coloring the modulation with more than one frequency [39,53–60]. We point out that synthetic gauge fields have also been realized in systems of transmons by suitable sets of two-qubit gates in the hardcore boson limit [61,62]. However, such investigations do not access the bright soliton physics determined by interactions.

In the next section, we propose a specific Floquet protocol that leads to generic Peierls phases in $\{0, 2\pi\}$ and that can also be employed with the transmons at the sweet spot. Our Floquet scheme employs the so-called Leviton dynamics.

III. SYNTHETIC GAUGE FIELD BY LEVITON PROTOCOL

Levitons consist of suitable Lorentzian pulses that are characterized by an exponential Fourier spectrum and yield a quantized phase advanced of 2π. Based on such a feature, Levitons have been originally introduced in quantum physics by Levitov as noise-free electronic excitations for edge states in the quantum Hall effect regimes [63–67]. Here, we propose Levitons to implement a synthetic gauge field by Floquet dynamics. The protocol consists in modulating a suitable subset of adjacent $N_m < N_s$ transmons through a sequence of Leviton pulses of period T and width τ:

$$\delta\omega_j(t) = \sum_k \frac{2\tau}{(t - t_j - kT)^2 + \tau^2}, \quad (3)$$

in which t_j is a site-dependent reference time. We shall see that $N_m \geqslant 2$ is a necessary condition for the protocol to work. Thanks to the properties of Levitons, it can be analytically shown that the hopping between the modulated adjacent transmons acquires a phase γ:

$$J e^{-i\gamma} = \langle J_0 e^{-i \int^t dt' (\delta\omega(t') - \delta\omega(t' - \delta t))} \rangle_T, \quad (4)$$

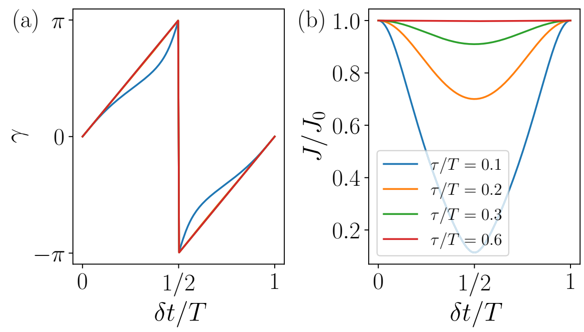

FIG. 2. (a) Phase and (b) modulus of the complex hopping between two transmons modulated through Levitons, as a function of the time delay $\delta t/T$ for four different values of the Lorentzian width τ/T [in panel (a), only the curve for the smallest width can be distinguished from the other three curves].

which can be adjusted by varying the time delay $\delta t = (t_{j+1} - t_j)$ between pulses in adjacent transmons. This feature can be explicitly seen for $e^{-4\pi\tau/T} \ll 1$ for which we have $Je^{-i\gamma} \simeq J_0 e^{-2\pi i\delta t/T}$ (see also the Supplemental Material [46]). Indeed, Fig. 2(a) shows an approximately linearly increasing phase γ between two adjacent transmons versus δt, for different values of the normalized Lorentzian width τ/T such that $e^{-4\pi\tau/T} \ll 1$. At the same time, the hopping rate J/J_0 is also shown to be weakly dependent on δt, as shown in Fig. 2(b).

We comment that, due to the linear dependence of the phase γ on δt, modulating all the transmons with time-shifted pulses does not lead to any synthetic flux (since all phases gained cancel out around the ring). In turn, by modulating only a subset of N_m transmons, a net synthetic flux can be achieved. This choice introduces two "external" links between the modulated and nonmodulated transmons, and the associated hopping rate J' is suppressed:

$$J' = \langle J_0 e^{-i\int^t dt'\delta\omega(t'-t_j)}\rangle_T = -J_0 e^{-2\pi\tau/T}. \quad (5)$$

Therefore, in order to preserve the translation invariance of the system in the fundamental Floquet band, the bare hopping at the external links needs to be modified to compensate the suppression due to the modulation, $J_0 \to J_0' = J_0 e^{2\pi\tau/T}$. Additionally, the π phase shift acquired in one external link is compensated by an analogous one at the second external link. The result of the protocol is that we can impart a net synthetic flux to the system

$$\Phi = 2\pi(N_m - 1)\delta t/T, \quad (6)$$

which can be controlled with the time delay of the pulses between adjacent transmons.

Several comments are now in order. (1) The Floquet protocol based on Leviton dynamics can interestingly be employed at the transmon sweet spots. To see this, we notice that the minimum of the modulation $\delta\omega(t)$ is $\omega_c = (2\pi/T)\tanh(\pi\tau/T)$ and when the transmons are modulated at the sweet spot they naturally generate a "dc component" ω_c [46]. (2) In order to utilize the series of Levitons at the sweet spots, it is then necessary to shift the frequency ω of the modulated transmons by ω_c, so to compensates the dc component. The proper value of the Floquet period T and the width of the Lorentzians τ can then be adjusted *a posteriori*, so to match the step ω_c and the bare hopping J_0'. (3) We note that the rescaling of J_0' breaks the original translation invariance of the Hamiltonian H_0 and can introduce coupling to higher Floquet bands in the exact time-dependent dynamics. Nevertheless, for sufficiently high Floquet frequency such that $2\pi/T \gg J_0' e^{2\pi\tau/T}$ these transitions can be suppressed [46]. (4) Finally, we point out that requiring the total amplitude of the modulation to be a fraction of the transmon frequency sets the correct hierarchy of frequency scales: $2\pi/T < 2\pi/\tau < \omega$. This is not in contrast with the requirement that the Floquet frequency is effectively the higher scale in the system as in each sector of constant number of bosons the dynamics is controlled by J/U; typical values of $J/\omega \sim 10^{-2}$ can fully justify a Floquet regime in which $J \ll 2\pi/T \ll \omega$. The numerical comparison between the target and the actual dynamics of the system is carried out in the Supplemental Material [46].

IV. SPECTRUM MEASUREMENT

Having established a protocol for imparting a synthetic flux to the system, we now propose an experimentally feasible scheme for detecting the effect of Φ on the superconducting circuit. Specifically, we consider a transmission line capacitively coupled to the ring of transmons and add the driving term $\Omega\cos(\omega_d t)(a_1 + a_1^\dagger)$ to the Hamiltonian, where Ω characterizes the strength of the driving. The ring network can then be coherently driven by microwaves of frequency ω_d and by the same transmission line the outgoing photons can be monitored. This way, we can map out the spectrum of the system through the amplitude of the reflected wave $S(\omega_d)$. Following Ref. [35] and by time averaging the combined Floquet modulation and external driving dynamics (in the rotating frame of the driving), the effective Hamiltonian becomes [46]

$$H_{\text{eff}} = \sum_{j=1}^{N_s}\left[(\omega - \omega_d)n_j - \frac{U}{2}n_j(n_j - 1)\right] - J_0\sum_{j=1}^{N_s}(e^{i\Phi/N_s}a_{j+1}^\dagger a_j + \text{H.c.}) + \frac{\Omega}{2}(a_1 + a_1^\dagger), \quad (7)$$

and we have neglected fast rotating terms for $\Omega \ll \omega$, ω_d. Clearly, the coherent driving implies non-number-conserving process (it couples sectors with different number of bosons): The system coherently absorbs photons from the transmission line and incoherently loses photons both via the transmission line and by relaxation processes in each transmon; in addition, dephasing in each transmon can also result in a loss of coherence. We expect that solitonic bands with different N_p are separated in energy by $\sim U$. Therefore, in order to avoid band mixing, we require $\Omega \ll U$. For simplicity, we assume that only transmons that are not modulated through the Floquet protocol are connected to the external drive.

We study the evolution of the entire system phenomenologically through a Lindblad master equation [68–71]

$$\frac{\partial\hat{\rho}}{\partial t} = \mathcal{L}[\hat{\rho}] = -i[H_{\text{eff}}, \hat{\rho}] + \mathcal{D}_1[\hat{\rho}] + \mathcal{D}_\phi[\hat{\rho}], \quad (8)$$

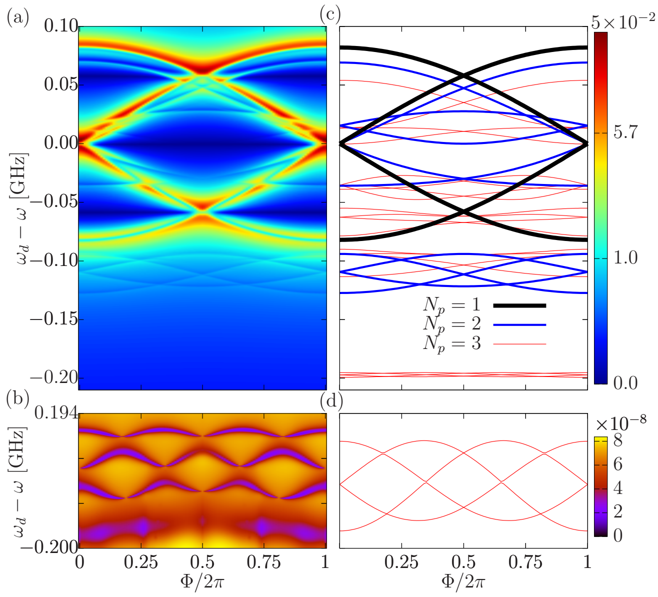

FIG. 3. (a) Modulus of the wave reflected off the driven system as a function of the synthetic flux Φ, detuning $\omega_d - \omega$ (in GHz), and driving amplitude $\Omega = 0.01$ GHz, for a chain of $N_s = 4$ transmons. A clear single-particle spectrum ($N_p = 1$) appears as a broad bright signal around zero detuning and shows the expected 2π periodicity as a function of the synthetic flux. At negative detuning, a band made of two-particle bound states characterizing bright solitons appears with the predicted periodicity halved to π (lower part of the spectra). (b) For further increasing the external drive $\Omega = 0.04$ GHz, three-particle bound states emerge with one-third periodicity. (c) Superimposed spectra of the $N_p = 1, 2, 3$ sectors, showing the correspondence with the output signal. (d) Close-up of the $N_p = 3$ sector. The rest of the system parameters are given in the main text. The color bar in panel (a) is made nonlinear by setting $z(x, y)^{2/5}$.

with $\mathcal{D}_\alpha[\hat{\rho}] = \sum_j [O_{j,(\alpha)}\hat{\rho}O^\dagger_{j,(\alpha)} - \frac{1}{2}\{O^\dagger_{j,(\alpha)}O_{j,(\alpha)}, \hat{\rho}\}]$ a general dissipator, which for relaxation processes is specified by $O_{j,(1)} = \sqrt{\gamma_1}a_j$ and for dephasing processes is described by $O_{j,(\phi)} = \sqrt{\gamma_\phi}a^\dagger_j a_j$, with γ_1 and γ_ϕ the transmon relaxation and pure dephasing rates, respectively, which within a phenomenological approach should be interpreted as effective ones. To model the system output, we follow Refs. [34,35,69] and assume that site 1 couples with rate Γ to the transmission line. Following a quantum Langevin approach [68,72,73], coherent irradiation results in the input field mode amplitude being related to the driving strength Ω as $\sqrt{\Gamma}\langle a^\dagger_{\rm in}\rangle \approx i\Omega$ and the output field is $a^\dagger_{\rm out} \approx \sqrt{\Gamma}a^\dagger_1$. In this regime, photon reflection amplitude is then expressed as

$$S(\omega_d) = \langle a^\dagger_{\rm out}\rangle/\langle a^\dagger_{\rm in}\rangle = \Gamma {\rm Tr}[\hat{\rho}_{ss}a^\dagger_1]/i\Omega \tag{9}$$

where $\hat{\rho}_{ss}$ is the steady-state density matrix satisfying $\partial\hat{\rho}_{ss}/\partial t = 0$. We then perform numerical simulations for system of size $N_s = 4$, keeping up to $N_p = 3$ excitations, and we choose experimentally relevant parameters taken from Ref. [35]: $\omega = 3.9$ GHz, $U = 0.188$ GHz, $J = 0.041$ GHz.

In Fig. 3(a), we present the results for weak driving $\Omega = 0.01$ GHz, $\Gamma = 5$ MHz, $\gamma_1 = 1$ MHz, and we neglect γ_ϕ (see Ref. [46] for a discussion of the role of γ_ϕ). Notice that typical decoherence rates are dominated by relaxation processes and that the chosen value of γ_1 is a worst-case scenario rather than an optimistic value. A clear broad bright signal following the dispersion $E^{(1)}_k = \omega - \omega_d - J\cos(2\pi k/N_s + \Phi/N_s)$, for $k = 0, \ldots, N_s - 1$ emerges. This feature, displaying the full 2π flux periodicity, is identified as corresponding to the $N_p = 1$ sector. Remarkably, a weaker signal in the form of a dip is visible, in the lower part of Fig. 3(a), which corresponds to the $N_p = 2$ sector. Here, we see the inception of the reduced periodicity, where a minimum appears between $\Phi = 0$ and $\Phi = 2\pi$. The apparent deviations with respect to the perfect reduced periodicity were demonstrated to arise as $1/N_s$ corrections [18,21,74]. In order to observe the $N_p = 3$ bound state, we needed to increase the driving amplitude Ω to be of order J. We comment that the timescale for photon hopping from the transmission line to the lattice site $j = 1$, determined by $2\pi/\Omega$, has to be comparable to or shorter than the timescale on which photons hop from one transmon to the other, $1/J$, requiring $\Omega \gtrsim J$. For $\Omega = 0.04$ GHz, $\Gamma = 0.1$ MHz, and $\gamma_1 = 10^{-2}$ MHz, the sector $N_p = 3$ appears, as shown in Fig. 3(b). The lowest energy band is displayed as significantly broadened and we can only observe the fractional $2\pi/3$ periodicity in the excited bands. We also point out that degeneracies in the level crossings of the many-body spectrum, taking place at specific values of the synthetic flux, are lifted as a combined effect of driving and dissipation.

Our numerical findings are corroborated by a perturbative calculation valid for large U of the energy dispersion [46]

$$E^{(N_p)}_k = E^{(N_p)}_0 - J_{(N_p)}\cos(2\pi k/N_s + N_p\Phi/N_s), \tag{10}$$

with $E^{(N_p)}_0 = N_p(\omega - \omega_d) - \frac{U}{2}N_p(N_p - 1)$ and $J_{(N_p)} = \frac{JN_p}{(N_p-1)!}(J/U)^{N_p-1}$ [75]. This formula is in good agreement with the exact spectrum shown in Figs. 3(c) and 3(d).

In summary, our analysis shows that the low energy bands in the absorption spectrum have a periodicity reduced by N_p reflecting the size of the bound state formed in the system. According to the predictions in Ref. [18], for sufficiently strong attractive interactions the energy bands corresponding to bound states detach from the single particle (scattering) band [see Fig. 3(c)]. We note that solitons are increasingly more fragile with N_p to decoherence. This is due to the fact that the solitons take approximately a time $\sim N_s/J_{(N_p)}$ to go around the ring of transmons. Therefore, to observe coherent flux oscillations such a time has to be shorter than the single transmon relaxation time $\sim 1/(N_p\gamma_1)$ and pure dephasing time $1/\gamma_\phi$ [76]. Thus, we require $N_p\gamma_1$, $\gamma_\phi \ll J_{(N_p)}/N_s$, so that the protocol needs a ratio J/U not too small. The chosen value of the relaxation rate in Fig. 3(b) is within the state-of-the-art values [77,78] and we have checked that the solitons and their periodicity are visible up to $\gamma_1 = 0.1$ MHz (see Ref. [46] for an assessment of the coherence properties).

V. CONCLUSIONS

We have shown how a ring-shaped system of capacitively coupled transmons can be employed to study the many-body dynamics of attracting bosons in the presence of an effective magnetic field. The latter is obtained through a suitable

Floquet driving protocol employing Lorentzian pulses (Levitons). This way, we widen the scope of the superconducting circuit quantum simulators significantly.

The bosonic effective dynamics is indeed characterized by the formation of bright solitons whose smoking gun is the fractionalization of flux quantum that is predicted to be displayed in the "band structure" of the system (energy versus magnetic field) [18,21]. Such flux quantum fractionalization emerges for realistic experimental conditions [35] in a suitable reflection protocol (see Fig. 3).

Important problems such as the impact of disorder on the fractionalization, macroscopic phase coherence and SQUID physics [37], Aharonov-Bohm oscillations in bosonic systems [79], N-component bosons, and mesoscopic simulation of lattice gauge theories [80] can be studied in a regime of parameters that is complementary to the working conditions of strongly interacting cold atom systems. Such a platform is also complementary to others describing synthetic gauge fields in weakly coupled photons, such as those occurring in topological photonics [81]. Relying on the relevance of solitons in quantum metrology [19,82–85], we expect that our scheme can open perspectives for superconducting circuit-based quantum sensing.

ACKNOWLEDGMENT

We thank B. Blain, E. C. Domanti, and G. Marchegiani for discussions.

DATA AVAILABILITY

The data that support the findings of this article are not publicly available. The data are available from the authors upon reasonable request.

[1] Y. Imry, *Introduction to Mesoscopic Physics* (Oxford University Press, New York, 2002).

[2] P. Michler, *Quantum Dots for Quantum Information Technologies* (Springer, Cham, 2017), Vol. 237.

[3] L.-M. Duan and C. Monroe, *Colloquium*: Quantum networks with trapped ions, Rev. Mod. Phys. **82**, 1209 (2010).

[4] M. Kjaergaard, M. E. Schwartz, J. Braumüller, P. Krantz, J. I.-J. Wang, S. Gustavsson, and W. D. Oliver, Superconducting qubits: Current state of play, Annu. Rev. Condens. Matter Phys. **11**, 369 (2020).

[5] I. Bloch, J. Dalibard, and S. Nascimbene, Quantum simulations with ultracold quantum gases, Nat. Phys. **8**, 267 (2012).

[6] D. Bluvstein, A. Omran, H. Levine, A. Keesling, G. Semeghini, S. Ebadi, T. T. Wang, A. A. Michailidis, N. Maskara, W. W. Ho *et al.*, Controlling quantum many-body dynamics in driven Rydberg atom arrays, Science **371**, 1355 (2021).

[7] S. Krinner, D. Stadler, D. Husmann, J.-P. Brantut, and T. Esslinger, Observation of quantized conductance in neutral matter, Nature (London) **517**, 64 (2015).

[8] G. Valtolina, A. Burchianti, A. Amico, E. Neri, K. Xhani, J. A. Seman, A. Trombettoni, A. Smerzi, M. Zaccanti, M. Inguscio, and G. Roati, Josephson effect in fermionic superfluids across the BEC-BCS crossover, Science **350**, 1505 (2015).

[9] V. P. Singh, J. Polo, L. Mathey, and L. Amico, Shapiro steps in driven atomic Josephson junctions, Phys. Rev. Lett. **133**, 093401 (2024).

[10] L. Amico, D. Anderson, M. Boshier, J.-P. Brantut, L.-C. Kwek, A. Minguzzi, and W. von Klitzing, Colloquium: Atomtronic circuits: From many-body physics to quantum technologies, Rev. Mod. Phys. **94**, 041001 (2022).

[11] L. Amico, M. Boshier, G. Birkl, A. Minguzzi, C. Miniatura, L.-C. Kwek, D. Aghamalyan, V. Ahufinger, D. Anderson, N. Andrei *et al.*, Roadmap on atomtronics: State of the art and perspective, AVS Quantum Sci. **3**, 039201 (2021).

[12] J. Polo, W. J. Chetcuti, E. C. Domanti, P. Kitson, A. Osterloh, F. Perciavalle, V. P. Singh, and L. Amico, Perspective on new implementations of atomtronic circuits, Quantum Sci. Technol. **9**, 030501 (2024).

[13] L. D. Carr, C. W. Clark, and W. P. Reinhardt, Stationary solutions of the one-dimensional nonlinear Schrödinger equation. II. Case of attractive nonlinearity, Phys. Rev. A **62**, 063611 (2000).

[14] K. E. Strecker, G. B. Partridge, A. G. Truscott, and R. G. Hulet, Formation and propagation of matter-wave soliton trains, Nature (London) **417**, 150 (2002).

[15] L. Khaykovich, F. Schreck, G. Ferrari, T. Bourdel, J. Cubizolles, L. D. Carr, Y. Castin, and C. Salomon, Formation of a matter-wave bright soliton, Science **296**, 1290 (2002).

[16] J. H. Nguyen, D. Luo, and R. G. Hulet, Formation of matter-wave soliton trains by modulational instability, Science **356**, 422 (2017).

[17] A. Marchant, T. Billam, T. Wiles, M. Yu, S. Gardiner, and S. Cornish, Controlled formation and reflection of a bright solitary matter-wave, Nat. Commun. **4**, 1865 (2013).

[18] P. Naldesi, J. P. Gomez, B. Malomed, M. Olshanii, A. Minguzzi, and L. Amico, Rise and fall of a bright soliton in an optical lattice, Phys. Rev. Lett. **122**, 053001 (2019).

[19] P. Naldesi, J. Polo, P. D. Drummond, V. Dunjko, L. Amico, A. Minguzzi, and M. Olshanii, Massive particle interferometry with lattice solitons, SciPost Phys. **15**, 187 (2023).

[20] A. J. Leggett, Dephasing and non-dephasing collisions in nanostructures, *Granular Nanoelectronics* (Springer US, Boston, MA, 1991), pp. 297–311.

[21] P. Naldesi, J. Polo, V. Dunjko, H. Perrin, M. Olshanii, L. Amico, and A. Minguzzi, Enhancing sensitivity to rotations with quantum solitonic currents, SciPost Phys. **12**, 138 (2022).

[22] R. Ma, B. Saxberg, C. Owens, N. Leung, Y. Lu, J. Simon, and D. I. Schuster, A dissipatively stabilized Mott insulator of photons, Nature (London) **566**, 51 (2019).

[23] P. Roushan, C. Neill, J. Tangpanitanon, V. M. Bastidas, A. Megrant, R. Barends, Y. Chen, Z. Chen, B. Chiaro, A. Dunsworth *et al.*, Spectroscopic signatures of localization with interacting photons in superconducting qubits, Science **358**, 1175 (2017).

[24] K. Xu, J.-J. Chen, Y. Zeng, Y.-R. Zhang, C. Song, W. Liu, Q. Guo, P. Zhang, D. Xu, H. Deng, K. Huang, H. Wang, X. Zhu, D. Zheng, and H. Fan, Emulating many-body localization with

a superconducting quantum processor, Phys. Rev. Lett. **120**, 050507 (2018).

[25] Q. Guo, C. Cheng, Z.-H. Sun, Z. Song, H. Li, Z. Wang, W. Ren, H. Dong, D. Zheng, Y.-R. Zhang *et al.*, Observation of energy-resolved many-body localization, Nat. Phys. **17**, 234 (2021).

[26] B. Chiaro, C. Neill, A. Bohrdt, M. Filippone, F. Arute, K. Arya, R. Babbush, D. Bacon, J. Bardin, R. Barends *et al.*, Direct measurement of nonlocal interactions in the many-body localized phase, Phys. Rev. Res. **4**, 013148 (2022).

[27] O. Mansikkamäki, S. Laine, and M. Silveri, Phases of the disordered Bose-Hubbard model with attractive interactions, Phys. Rev. B **103**, L220202 (2021).

[28] Z. Yan, Y.-R. Zhang, M. Gong, Y. Wu, Y. Zheng, S. Li, C. Wang, F. Liang, J. Lin, Y. Xu *et al.*, Strongly correlated quantum walks with a 12-qubit superconducting processor, Science **364**, 753 (2019).

[29] M. K. Giri, S. Mondal, B. P. Das, and T. Mishra, Two component quantum walk in one-dimensional lattice with hopping imbalance, Sci. Rep. **11**, 22056 (2021).

[30] X. Zhang, E. Kim, D. K. Mark, S. Choi, and O. Painter, A superconducting quantum simulator based on a photonic-bandgap metamaterial, Science **379**, 278 (2023).

[31] X. Li, Y. Ma, J. Han, T. Chen, Y. Xu, W. Cai, H. Wang, Y. Song, Z.-Y. Xue, Z.-q. Yin, and L. Sun, Perfect quantum state transfer in a superconducting qubit chain with parametrically tunable couplings, Phys. Rev. Appl. **10**, 054009 (2018).

[32] F. A. Roy, J. H. Romeiro, L. Koch, I. Tsitsilin, J. Schirk, N. J. Glaser, N. Bruckmoser, M. Singh, F. X. Haslbeck, G. B. P. Huber, G. Krylov, A. Marx, F. Pfeiffer, C. M. F. Schneider, C. Schweizer, F. Wallner, D. Bunch, L. Richard, L. Södergren, K. Liegener *et al.*, Parity-dependent state transfer for direct entanglement generation, Nat Commun **16**, 2660 (2025).

[33] R. Fazio and H. Van Der Zant, Quantum phase transitions and vortex dynamics in superconducting networks, Phys. Rep. **355**, 235 (2001).

[34] S. Hacohen-Gourgy, V. V. Ramasesh, C. De Grandi, I. Siddiqi, and S. M. Girvin, Cooling and autonomous feedback in a Bose-Hubbard chain with attractive interactions, Phys. Rev. Lett. **115**, 240501 (2015).

[35] G. P. Fedorov, S. V. Remizov, D. S. Shapiro, W. V. Pogosov, E. Egorova, I. Tsitsilin, M. Andronik, A. A. Dobronosova, I. A. Rodionov, O. V. Astafiev, and A. V. Ustinov, Photon transport in a Bose-Hubbard chain of superconducting artificial atoms, Phys. Rev. Lett. **126**, 180503 (2021).

[36] J. Polo, P. Naldesi, A. Minguzzi, and L. Amico, Exact results for persistent currents of two bosons in a ring lattice, Phys. Rev. A **101**, 043418 (2020).

[37] J. Polo, P. Naldesi, A. Minguzzi, and L. Amico, The quantum solitons atomtronic interference device, Quantum Sci. Technol. **7**, 015015 (2022).

[38] B. Blain, G. Marchegiani, J. Polo, G. Catelani, and L. Amico, Soliton versus single-photon quantum dynamics in arrays of superconducting qubits, Phys. Rev. Res. **5**, 033130 (2023).

[39] A. Eckardt, C. Weiss, and M. Holthaus, Superfluid-insulator transition in a periodically driven optical lattice, Phys. Rev. Lett. **95**, 260404 (2005).

[40] Y. J. Lin, R. L. Compton, K. Jiménez-García, J. V. Porto, and I. B. Spielman, Synthetic magnetic fields for ultracold neutral atoms, Nature (London) **462**, 628 (2009).

[41] A. R. Kolovsky, Creating artificial magnetic fields for cold atoms by photon-assisted tunneling, Europhys. Lett. **93**, 20003 (2011).

[42] G. Jotzu, M. Messer, R. Desbuquois, M. Lebrat, T. Uehlinger, D. Greif, and T. Esslinger, Experimental realization of the topological Haldane model with ultracold fermions, Nature (London) **515**, 237 (2014).

[43] H.-T. Lim, E. Togan, M. Kroner, J. Miguel-Sanchez, and A. Imamoğlu, Electrically tunable artificial gauge potential for polaritons, Nat. Commun. **8**, 14540 (2017).

[44] T. Orell, A. A. Michailidis, M. Serbyn, and M. Silveri, Probing the many-body localization phase transition with superconducting circuits, Phys. Rev. B **100**, 134504 (2019).

[45] T. Orell, M. Zanner, M. L. Juan, A. Sharafiev, R. Albert, S. Oleschko, G. Kirchmair, and M. Silveri, Collective bosonic effects in an array of transmon devices, Phys. Rev. A **105**, 063701 (2022).

[46] See Supplemental Material at http://link.aps.org/supplemental/10.1103/d3rk-kh1k for details on the circuit, on the driving protocol, and on the driven-dissipative dynamics.

[47] L. Chirolli and G. Burkard, Decoherence in solid-state qubits, Adv. Phys. **57**, 225 (2008).

[48] P. Krantz, M. Kjaergaard, F. Yan, T. P. Orlando, S. Gustavsson, and W. D. Oliver, A quantum engineer's guide to superconducting qubits, Appl. Phys. Rev. **6**, 021318 (2019).

[49] I. Siddiqi, Engineering high-coherence superconducting qubits, Nat. Rev. Mater. **6**, 875 (2021).

[50] R. Peierls, On the theory of the diamagnetism of conduction electrons, in *Selected Scientific Papers of Sir Rudolf Peierls (With Commentary)* (World Scientific, 1997), pp. 97–120.

[51] I. T. Rosen, S. Muschinske, C. N. Barrett, A. Chatterjee, M. Hays, M. A. DeMarco, A. H. Karamlou, D. A. Rower, R. Das, D. K. Kim, B. M. Niedzielski, M. Schuldt, K. Serniak, M. E. Schwartz, J. L. Yoder, J. A. Grover, and W. D. Oliver, A synthetic magnetic vector potential in a 2D superconducting qubit array, Nat. Phys. **20**, 1881 (2024).

[52] I. T. Rosen, S. Muschinske, C. N. Barrett, D. A. Rower, R. Das, D. K. Kim, B. M. Niedzielski, M. Schuldt, K. Serniak, M. E. Schwartz, J. L. Yoder, J. A. Grover, and W. D. Oliver, Flat-band (de)localization emulated with a superconducting qubit array, Phys. Rev. X **15**, 021091 (2025).

[53] D. H. Dunlap and V. M. Kenkre, Dynamic localization of a charged particle moving under the influence of an electric field, Phys. Rev. B **34**, 3625 (1986).

[54] F. Grossmann and P. Hanggi, Localization in a driven two-level dynamics, Europhys. Lett. **18**, 571 (1992).

[55] M. Holthaus, Collapse of minibands in far-infrared irradiated superlattices, Phys. Rev. Lett. **69**, 351 (1992).

[56] J. Struck, C. Ölschläger, M. Weinberg, P. Hauke, J. Simonet, A. Eckardt, M. Lewenstein, K. Sengstock, and P. Windpassinger, Tunable gauge potential for neutral and spinless particles in driven optical lattices, Phys. Rev. Lett. **108**, 225304 (2012).

[57] S. Flach, O. Yevtushenko, and Y. Zolotaryuk, Directed current due to broken time-space symmetry, Phys. Rev. Lett. **84**, 2358 (2000).

[58] S. Denisov, L. Morales-Molina, S. Flach, and P. Hänggi, Periodically driven quantum ratchets: Symmetries and resonances, Phys. Rev. A **75**, 063424 (2007).

[59] A. Verdeny, Ł. Rudnicki, C. A. Müller, and F. Mintert, Optimal control of effective Hamiltonians, Phys. Rev. Lett. **113**, 010501 (2014).

[60] T. W. Borneman, M. D. Hürlimann, and D. G. Cory, Application of optimal control to CPMG refocusing pulse design, J. Magn. Reson. **207**, 220 (2010).

[61] C. Neill, T. McCourt, X. Mi, Z. Jiang, M. Y. Niu, W. Mruczkiewicz, I. Aleiner, F. Arute, K. Arya, J. Atalaya *et al.*, Accurately computing the electronic properties of a quantum ring, Nature (London) **594**, 508 (2021).

[62] A. Morvan, T. I. Andersen, X. Mi, C. Neill, A. Petukhov, K. Kechedzhi, D. A. Abanin, A. Michailidis, R. Acharya, F. Arute *et al.*, Formation of robust bound states of interacting microwave photons, Nature (London) **612**, 240 (2022).

[63] L. S. Levitov, H. Lee, and G. B. Lesovik, Electron counting statistics and coherent states of electric current, J. Math. Phys. **37**, 4845 (1996).

[64] D. A. Ivanov, H. W. Lee, and L. S. Levitov, Coherent states of alternating current, Phys. Rev. B **56**, 6839 (1997).

[65] J. Keeling, I. Klich, and L. S. Levitov, Minimal excitation states of electrons in one-dimensional wires, Phys. Rev. Lett. **97**, 116403 (2006).

[66] J. Dubois, T. Jullien, F. Portier, P. Roche, A. Cavanna, Y. Jin, W. Wegscheider, P. Roulleau, and D. C. Glattli, Minimal-excitation states for electron quantum optics using levitons, Nature (London) **502**, 659 (2013).

[67] D. C. Glattli and P. S. Roulleau, Levitons for electron quantum optics, Phys. Status Solidi B **254**, 1600650 (2017).

[68] H. P. Breuer and F. Petruccione, *The Theory of Open Quantum Systems* (Clarendon Press, Oxford, 2002).

[69] A. Biella, L. Mazza, I. Carusotto, D. Rossini, and R. Fazio, Photon transport in a dissipative chain of nonlinear cavities, Phys. Rev. A **91**, 053815 (2015).

[70] R. Fazio, J. Keeling, L. Mazza, and M. Schirò, Many-body open quantum systems, SciPost Phys. Lect. Notes 99 (2025).

[71] J. Venkatraman, X. Xiao, R. G. Cortiñas, and M. H. Devoret, Nonlinear dissipation in a driven superconducting circuit, Phys. Rev. A **110**, 042411 (2024).

[72] M. J. Collett and C. W. Gardiner, Squeezing of intracavity and traveling-wave light fields produced in parametric amplification, Phys. Rev. A **30**, 1386 (1984).

[73] M. Mirhosseini, E. Kim, X. Zhang, A. Sipahigil, P. B. Dieterle, A. J. Keller, A. Asenjo-Garcia, D. E. Chang, and O. Painter, Cavity quantum electrodynamics with atom-like mirrors, Nature (London) **569**, 692 (2019).

[74] L. Piroli and P. Calabrese, Local correlations in the attractive one-dimensional Bose gas: From Bethe ansatz to the Gross-Pitaevskii equation, Phys. Rev. A **94**, 053620 (2016).

[75] O. Mansikkamäki, S. Laine, A. Piltonen, and M. Silveri, Beyond hard-core bosons in transmon arrays, PRX Quantum **3**, 040314 (2022).

[76] M. J. Peterer, S. J. Bader, X. Jin, F. Yan, A. Kamal, T. J. Gudmundsen, P. J. Leek, T. P. Orlando, W. D. Oliver, and S. Gustavsson, Coherence and decay of higher energy levels of a superconducting transmon qubit, Phys. Rev. Lett. **114**, 010501 (2015).

[77] O. Milul, B. Guttel, U. Goldblatt, S. Hazanov, L. M. Joshi, D. Chausovsky, N. Kahn, E. Çiftyürek, F. Lafont, and S. Rosenblum, Superconducting cavity qubit with tens of milliseconds single-photon coherence time, PRX Quantum **4**, 030336 (2023).

[78] S. Ganjam, Y. Wang, Y. Lu, A. Banerjee, C. U. Lei, L. Krayzman, K. Kisslinger, C. Zhou, R. Li, Y. Jia, M. Liu, L. Frunzio, and R. J. Schoelkopf, Surpassing millisecond coherence in on chip superconducting quantum memories by optimizing materials and circuit design, Nat. Commun. **15**, 3687 (2024).

[79] T. Haug, H. Heimonen, R. Dumke, L.-C. Kwek, and L. Amico, Aharonov-Bohm effect in mesoscopic Bose-Einstein condensates, Phys. Rev. A **100**, 041601 (2019).

[80] E. C. Domanti, P. Castorina, D. Zappalà, and L. Amico, Aharonov-Bohm effect for confined matter in lattice gauge theories, Phys. Rev. Res. **6**, 013268 (2024).

[81] T. Ozawa, H. M. Price, A. Amo, N. Goldman, M. Hafezi, L. Lu, M. C. Rechtsman, D. Schuster, J. Simon, O. Zilberberg, and I. Carusotto, Topological photonics, Rev. Mod. Phys. **91**, 015006 (2019).

[82] S. Cornish, N. Parker, A. Martin, T. Judd, R. Scott, T. Fromhold, and C. Adams, Quantum reflection of bright matter-wave solitons, Physica D **238**, 1299 (2009).

[83] G. D. McDonald, C. C. N. Kuhn, K. S. Hardman, S. Bennetts, P. J. Everitt, P. A. Altin, J. E. Debs, J. D. Close, and N. P. Robins, Bright solitonic matter-wave interferometer, Phys. Rev. Lett. **113**, 013002 (2014).

[84] J. L. Helm, S. L. Cornish, and S. A. Gardiner, Sagnac interferometry using bright matter-wave solitons, Phys. Rev. Lett. **114**, 134101 (2015).

[85] A. L. Marchant, T. P. Billam, M. M. H. Yu, A. Rakonjac, J. L. Helm, J. Polo, C. Weiss, S. A. Gardiner, and S. L. Cornish, Quantum reflection of bright solitary matter waves from a narrow attractive potential, Phys. Rev. A **93**, 021604 (2016).